ELSEVIER

Thermochimica Acta 399 (2003) 127–137

thermochimica acta

www.elsevier.com/locate/tca

Reaction kinetics and morphological changes of a rigid polyurethane foam during combustion

Carmen Branca [a], Colomba Di Blasi [a,*], Angela Casu [b], Vincenza Morone [b], Caterina Costa [b]

[a] *Dipartimento di Ingegneria Chimica, Universitá degli Studi di Napoli "Federico II", P.le V. Tecchio, 80125 Napoli, Italy*
[b] *ISRIM, Loc. Pentima Bassa 21, 05100 Terni, Italy*

Abstract

A three-step series mechanism is shown to provide a good description of the oxidative degradation of a rigid polyurethane foam. Kinetic constants have been estimated by the simultaneous evaluations of four weight loss curves measured for heating rates between 5 and 20 K/min and a final temperature of 873 K. The following parameters have been obtained for the three reaction steps: (I) $A_1 = 2.6\times10^{12}\,s^{-1}$, $E_1 = 133.6$ kJ/mol; (II) $A_2 = 3.3\times10^{4}\,s^{-1}$, $E_2 = 81$ kJ/mol; (III) $A_3 = 8.7\times10^{8}\,s^{-1}$, $E_3 = 180$ kJ/mol. The thermal response of the foam has also been examined in a cone calorimeter for low (25 kW/m^2) and high (50 kW/m^2) radiation intensities, which lead to flaming combustion for a period of 90 and 75s, respectively. In the latter case, a transition from flaming to slow smoldering also takes place. Finally, for both radiation intensities, SEM micrographs show the complete loss of the initial closed-cell structure.

Keywords: Rigid polyurethane foam; Kinetics; Combustion

1. Introduction

Polyurethanes are usually made by reacting polyisocyanates with polyols in the presence of a catalyst, whose nature depends on the desired characteristics of the product to be formed [1]. Flexible polyurethane foams are used predominantly in furniture, carpet underlay and bedding; semi-flexible foams in motor vehicles; rigid foams mainly in buildings and insulated appliances, such as refrigerators, tank and pipe insulation, etc. [2]. Thermal and oxidative decomposition of this class of polymers is of great importance in fire safety science and chemical reaction engineering, in relation to the performances and the disposal, respectively, of the material during and at the conclusion of its life cycle.

The large surface to volume ratio and the high permeability to gas flow make polyurethanes susceptible to smoldering combustion [3]. This is the combustion without flame in a porous medium in which heat is released by oxidation of the solid [4]. Though smolder is usually a slow process, it is of paramount importance in fire safety because of the toxicity of the evolved products, the difficulty of detection and the possibility of fire initiation through transition to flaming [5]. On the other hand, when the material has to be disposed off, the development and optimization of chemical reactors applied for combustion/gasification is based on the knowledge of the thermal characteristics and the reaction kinetics.

* Corresponding author. Tel.: +39-8176-82232; fax: +39-8123-91800.
E-mail address: diblasi@unina.it (C. Di Blasi).

0040-6031/02/$ – see front matter
PII: S0040-6031(02)00455-0

An extensive literature about the decomposition of polyurethanes is available, but only a few studies concern commercial foams [6]. In some cases, the focus of the research has been the coupling between the transport equations and the combustion kinetics, in other cases, thermogravimetric analysis has been used to formulate reaction mechanisms only.

The first group of analyses includes the treatment used in [7] and those initiated by Dosanjh et al. [8] and successively applied in other investigations (for instance, in [9]) for flexible polyurethane foams. In the former case [7], a two-step mechanism was considered consisting of the oxidative degradation of the fuel to produce char and the subsequent oxidation of char (activation energies of 140 and 126 kJ/mol, respectively). Based on the consideration that the rate of the reaction of char oxidation is much faster than that of the oxidative decomposition of the fuel (to give char), Dosanjh et al. [8] simplified the description of the process by means of a one-step reaction for the complete combustion of the polyurethane (activation energy of 155 kJ/mol).

The second group of studies [2,6,10,11] has been devoted to the determination of the decomposition kinetics of different polyurethanes through the aid of thermogravimetric analysis, in some cases, also with the identification of the volatile compounds generated [2,11]. Decomposition has been observed to be a multi-step process, reflecting the behavior of the single components, though interaction is considered responsible for the details of weight loss characteristics and the nature of evolved products [6].

Esperanza et al. [2] studied the decomposition in an inert atmosphere of varnish wastes based on a polyurethane. Two main peaks (reaction zones) in the devolatilization rate were observed. However, a mechanism based on three parallel reactions, with a power law dependence on the solid mass fractions, was required to describe with sufficient accuracy measurements carried out at different heating rates (activation energies of 89.5, 186.6 and 341 kJ/mol). Successively, the application of a two-step parallel reaction model was successfully accomplished by Font et al. [11] for the interpretation of the decomposition characteristics of a polyurethane used as a constituent of adhesives (activation energies of 133.6 and 190.4 kJ/mol).

The influences of the reaction atmosphere and the experimental procedure on the decomposition of polyurethane were investigated in [10]. In both nitrogen and air, isothermal measurements showed two different slopes in the Arrhenius plot, indicative of at least a two-step process. Process dynamics showed higher conversion in air, probably caused by a facilitation in the breakage of the polymeric chain, but the final conversion was the same. Furthermore, kinetic constants were estimated for a dynamic experiment in nitrogen (activation energies of 29, 63 and 180 kJ/mol for three successive reaction zones) and air (activation energy of 87 kJ/mol only for the central reaction zone).

As the reaction mechanisms and the related kinetic constants are significantly affected by the specific composition of the polyurethanes and the reaction atmosphere, prior to the development and validation of a transport model of smoldering combustion, a specific commercial polyurethane foam has been selected in order to determine the basic data of the process. The scarce information about the multi-step decomposition in air of this class of materials has motivated the first part of this study, dealing with the kinetic analysis of thermogravimetric curves measured at several heating rates. Relations for the thermal properties, highly affected by physical changes occurring during combustion, and measurments carried out under heat/mass transfer control are also needed. Information is provided in the second part of this study by means of an analysis of the thermal response and the morphological changes of thick samples radiatively heated.

2. Experimental

The material under study is a rigid polyurethane foam with the commercial name of polyurethane VORACOR (polyol C549 and isocyanate CD526 with proportion 100/110, Dow Chemical Company). The apparent density is 38 kg/m^3. Scanning electron microscope (SEM) photography (Fig. 1A and B) shows a structure consisting of void cells polygonally shaped with variable sizes (side about 200 μm). The cell surface frequently presents local gathers and deep voids about 800 μm wide (Fig. 1A and B). Practical applications of this commercial product include refrigerator cabinets, deep freeze panels and sandwich panels.

Thermogravimetric tests have been carried out in triplicate. Prior to decomposition, the polyurethane has

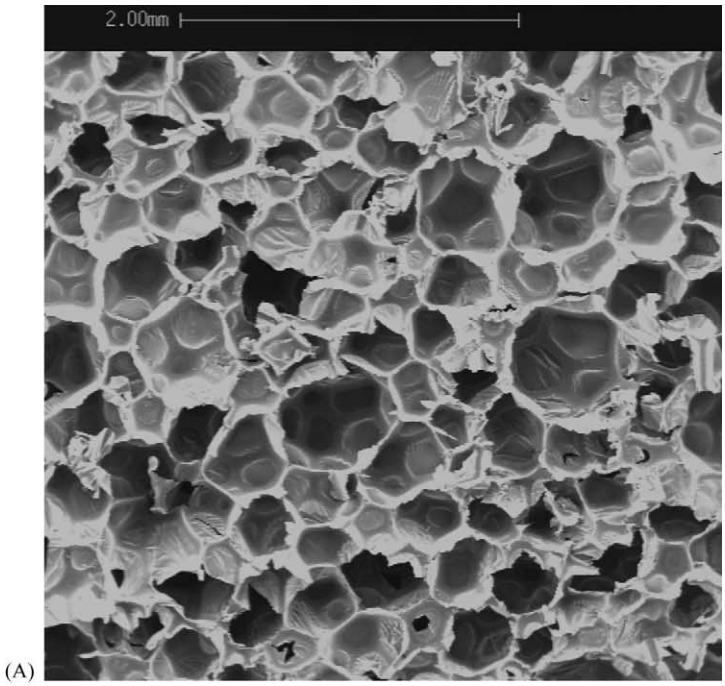

(A)

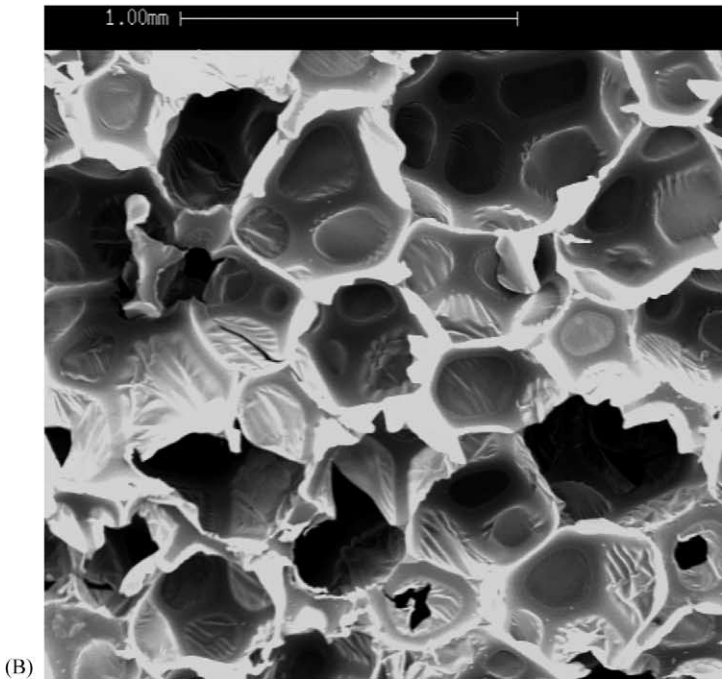

(B)

Fig. 1. (A) SEM micrographs of the polyurethane foam (20×). (B) SEM micrographs of the polyurethane foam (40×).

been prepared in the form of strips with a thickness below 400 μm (about 6 mg). The experimental system has been already presented elsewhere [12–14] and only the main characteristics are discussed here. It consists of a furnace, a quartz reactor, a PID controller, a gas feeding system, an acquisition data set, and a precision balance. The furnace is a radiant chamber, which creates a uniformly heated zone, where a quartz reactor is located. The sample is exposed to thermal radiation by means of a stainless steel mesh screen, whose sides are wrapped on two stainless steel rods connected to a precision (0.1 mg) balance, which allows the weight of the sample to be continously recorded. A gas flow (nominal velocity of 0.5×10^{-2} m/s for the tests discussed in this study) establishes the proper reaction environment and reduces the residence time of vapors inside the reactor.

For the tests presented here, the radiative heat flux emitted by the furnace is pre-registered imposing a certain heating rate of the sample holder (without sample). A chromel–alumel thermocouple (75 μm bead), positioned into direct physical contact with the sample, is then used to evaluate the temperature deviations with respect to the assigned heating rate. It has been observed that these are small for heating rates below 20 K/min, given a final temperature of 873 K. Hence, four measurements have been made for 5, 10, 15 and 20 K/min.

In order to evaluate the thermal response of the material and to investigate the morphological changes during combustion, a second set of tests has been carried out through a cone calorimeter system in accordance with ASTM 1354-1992. It is an oxygen consumption calorimeter [16] and the method is based on the assumptions that the specimen burns along the irradiance exposed surface and the net heat of combustion is proportional to the amount of oxygen required. The specimen is a 100 mm square sample exposed to a constant radiative heat flux. The pyrolysis gases are ignited by a spark, whereas combustion gases are extracted through an exhaust system. On-line measurements are carried out of oxygen, carbon monoxide and carbon dioxide concentrations, mass loss and attenuation of a (He–Ne) light beam (for smoke density). They also permit the evaluation of the heat release rate as a function of time (by means of the oxygen concentration), the effective heat of combustion (which takes into account the amount of solid burned) and the total heat evolved during the combustion process.

In this study specimen 32 mm thick have been horizontally exposed to radiation intensities, Q, equal to 25 and 50 kW/m^2. Again each test has been made in triplicate.

3. Results

In the first part, a kinetic mechanism and the related kinetic constants are presented for polyurethane degradation in air. The second part discusses the results of the cone calorimeter tests and shows the morphological changes undergone by the material.

3.1. Decomposition characteristics and reaction kinetics

Fig. 2 reports the solid mass fractions and the devolatilization rate of the polyurethane foam in air for a heating rate equal to 5 K/min (the temperature profile is also plotted). Three main reaction zones are evidenced by the peaks in the devolatilization rate. Decomposition starts at temperatures of about 435K (the initial decomposition temperature, T_i, corresponds to a solid mass fraction equal to 0.99) while the first peak rate is attained for a temperature (T_{m1}) of about 592 K. The amount of gases released is relatively small (about 8%). The other two reaction zones, which

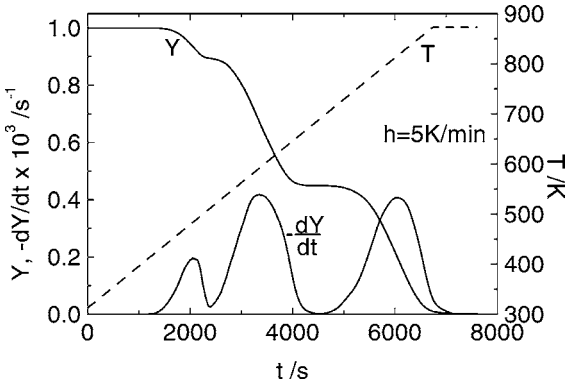

Fig. 2. Solid mass fraction, Y, time derivative of the solid mass fraction, $-\mathrm{d}Y/\mathrm{d}t$, and programmed temperature, T, as functions of time for a nominal heating rate of 5 K/min and a final temperature of 873 K.

Table 1
Initial degradation temperature, T_i, peaks in the devolatilization rate, $-(dY/dt)_{m1}$, $-(dY/dt)_{m2}$, $-(dY/dt)_{m3}$ and corresponding temperatures, T_{m1}, T_{m2}, T_{m3}, as measured (exp) and simulated (sim)

h (K/min)	T_i (K)	$-(dY/dt)_{m1} \times 10^3$ (s^{-1})	T_{m1} (K)	$-(dY/dt)_{m2} \times 10^3$ (s^{-1})	T_{m2} (K)	$-(dY/dt)_{m3} \times 10^3$ (s^{-1})	T_{m3} (K)
5							
Exp	437	0.20	483	0.42	592	0.41	815
Sim	434	0.19	479	0.44	591	0.44	816
10							
Exp	464	0.25	487	0.78	612	0.78	827
Sim	463	0.29	487	0.82	612	0.84	827
15							
Exp	472	0.32	491	1.14	631	1.35	849
Sim	472	0.33	491	1.14	626	1.33	844
20							
Exp	477	0.34	494	1.50	633	1.73	857
Sim	480	0.35	502	1.50	635	1.76	849

lead to a complete conversion of the material, are responsible for the release of the remaining 38 and 50% of the solid, respectively. The peak rates are detected for temperatures of 592 K (T_{m2}) and 815K (T_{m3}).

The same characteristics are maintained as the heating rate is increased, though the separation between the different zones becomes less evident. Moreover, the peak rates and the corresponding temperatures become successively higher, as shown in Table 1. These results are in qualitative agreement with previous analyses [2,6,10,11] showing the presence of two or three reaction zones for polyurethane decomposition under the conditions of thermal analysis.

Three main reaction zones are also observed for polyurethane degradation in inert atmosphere. A comparison between nitrogen and air for slow heating rates (3 K/min) shows that differences are relatively small for the first two reaction zones (the first peak is unaltered and the second is delayed of 30K in nitrogen). The effects of oxygen are higher for the third zone, which is anticipated of about 55 K. This finding is in agreement with previous results [10,17], which report temperature differences of 70–75 K. In accordance with these studies, it can be postulated that oxygen exerts a small influence on the decomposition rate of polyurethane to diisocyanates and polyols, whereas it affects significantly the breakage of the polymeric chains.

Following the features of process dynamics, a mechanism for the oxidative decomposition of polyurethane is proposed consisting of three sequential reactions:

$$A \xrightarrow{K_1} \alpha B + (1-\alpha)V1, \quad \alpha B \xrightarrow{K_2} \beta C + (\alpha-\beta)V2, \quad \beta C \xrightarrow{K_3} \beta V3 \qquad \text{(a1–a3)}$$

In reactions (a1–a3), A is the polyurethane foam, B and C charred residues, $V1$, $V2$, $V3$ lumped species representative of volatile species, α and β stoichiometric coefficients (expressed as fractions of the total initial mass).

The rates of reactions (a1–a3) are assumed to present the usual Arrhenius dependence (A pre-exponential factor and E activation energy) on temperature and, in order to minimize the number of parameters in the fitting procedure, to be a linear function of the solid mass fraction, Y_i:

$$R_i = -K_i Y_i, \quad K_i = A_i \exp\left(-\frac{E_i}{RT}\right) \qquad (1\text{–}3)$$

The sample temperature, T, is a known function of time, t:

$$T = T_0 + ht \qquad (4)$$

where T_0 is the initial temperature and h is the heating rate.

The parameters to be estimated are the activation energies (E_1, E_2, E_3), the pre-exponential factors (A_1, A_2, A_3) and the stoichiometric coefficients (α, β). They are estimated through the numerical solution (implicit Euler method) of the mass conservation

Table 2
Activation energies and pre-exponential factors for the oxidative decomposition of a rigid polyurethane foam (reactions (a1–a3))

Reaction	E (KJ/mol)	A (s^{-1})
a1	133.6	2.55×10^{12}
a2	81.0	3.26×10^{4}
a3	180.0	8.70×10^{8}

equations and the application of a direct method for the minimization of the objective function. The details of the method have been already described elsewhere [15].

The parameter estimation procedure is applied for the simultaneous evaluation of four weight loss curves obtained for heating rates between 5 and 20 K/min, so that the compensation effect is avoided [18]. The minimization procedure based on the differential form of the objective function presents the interesting feature of capturing all the details of the experiments [19]. However, since small experimental errors in the computation of the derivative may result in incorrect kinetic data [18], the integral form is also used for a further improvement in the kinetic constants. The optimization procedure has been executed by requiring the same value of activation energy and pre-exponential factor for all the curves, whereas the stoichiometric coefficients have been allowed to vary with the heating rate. For comparison purposes, average values have also been considered.

The results of the kinetic analysis are summarized in Tables 2 and 3 and a comparison between predictions and measurements is given in Fig. 3 for the solid mass fraction and in Fig. 4A and B for the global devolatilization rate. Furthermore, a comparison between measured and predicted peak rates and corresponding temperatures can be made through Table 1. The agreement between measurements and

Table 3
Stoichiometric coefficients of the reactions (a1–a3) for the oxidative decomposition of a rigid polyurethane foam

h (K/min)	α	β
5	0.92	0.45
10	0.93	0.46
15	0.95	0.48
20	0.96	0.49
Average	0.94	0.47

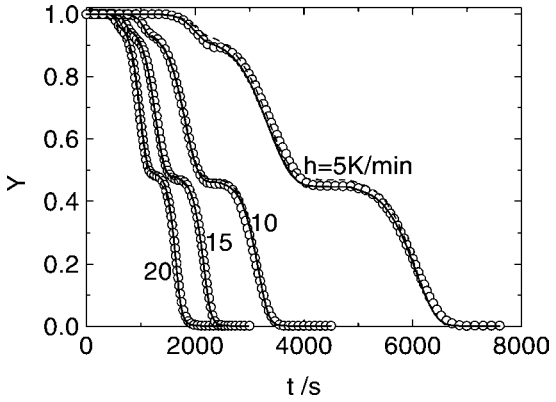

Fig. 3. Solid mass fractions, Y, as functions of time for heating rates of 5, 10, 15 and 20 K/min and a final temperature of 873 K, as predicted (Tables 2 and 3), with variable (solid lines) and average (dashed lines) values of the stoichiometric coefficients, and measured (symbols).

predictions is good when the stoichiometric coefficients are allowed to vary with the heating rate (maximum variations of 4%) or taken equal to the average values. It appears that the activity of reactions a2 and a3 begins for slightly increasing solid mass fractions as the heating rate is increased.

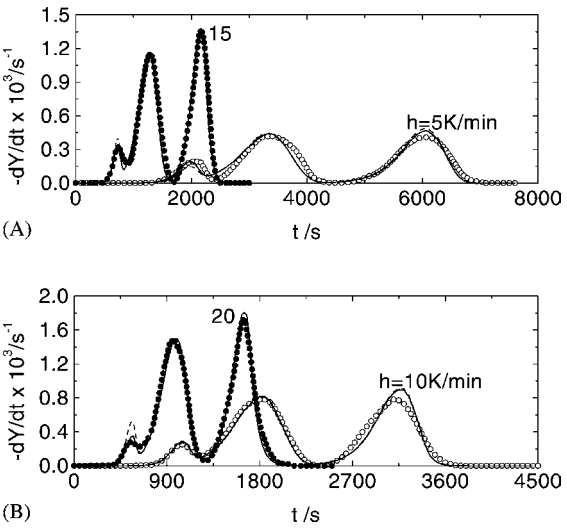

Fig. 4. Time derivatives of the mass fraction, $-\mathrm{d}Y/\mathrm{d}t$, as functions of time for heating rates of (A) 5 and 15 K/min, and (B) 10 and 20 K/min and a final temperature of 873 K, as predicted (Tables 2 and 3), with variable (solid lines) and average (dashed lines) values of the stoichiometric coefficients, and measured (symbols).

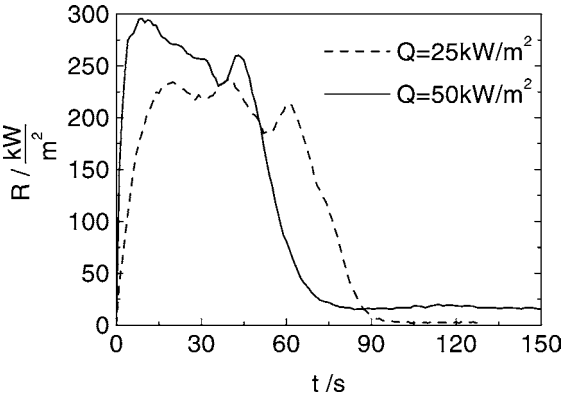

Fig. 5. Rate of heat release, R, as a function of time for two values of the applied radiative heat flux, Q, in a cone calorimeter.

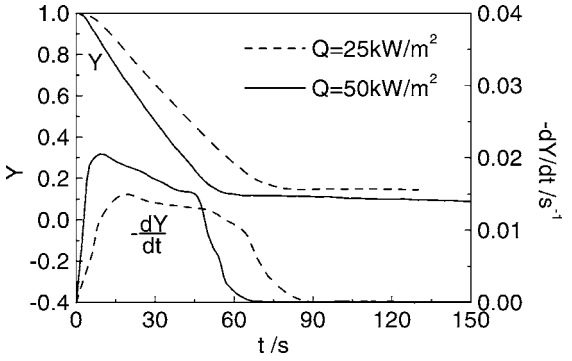

Fig. 6. Total solid mass fraction and time derivatives of the mass fraction as functions of time for two values of the applied radiative heat flux, Q, in a cone calorimeter.

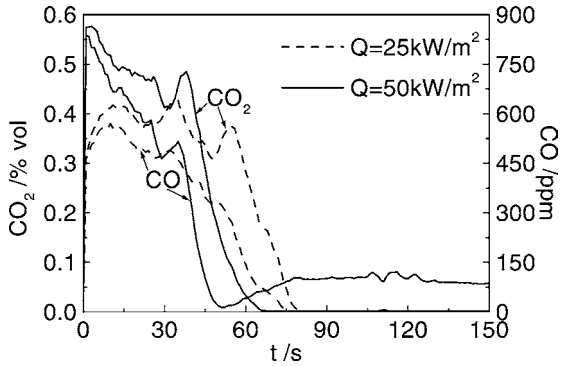

Fig. 7. Carbon monoxide and carbon dioxide concentrations as functions of time for two values of the applied radiative heat flux, Q, in a cone calorimeter.

The estimated activation energies (133.6, 81 and 180 kJ/mol) are in the range of literature values. Though quantitative comparisons are difficult because of the different sample properties, it is worth noting that the characteristics of the first step observed in this study and in [11] are very similar. Indeed, reference [11] reports an amount of gases evolved of 10% (against 8–4% of this study) and the same activation energy (133.6 kJ/mol).

3.2. Thermal response of thick samples

Figs. 5–7 summarize the results obtained from the cone calorimeter tests in terms of heat release rate, solid mass fraction, rate of weight loss and carbon monoxide and carbon dioxide concentrations for Q equal to 25 and 50 kW/m^2. Also, Table 4 reports the values (averaged over three tests) of several process parameters for the two radiation intensities. The time to ignition is the same for both cases, because the beginning of gaseous species evolution is almost instantaneous, soon after followed by the attainment of a peak in the rate of heat release, R. As expected, the peaks in the variable R, species concentrations and rate of mass loss are higher for the higher external heat flux. The duration of flaming combustion takes about 90 and 75 s for Q equal to 25 and 50 kW/m^2, respectively (the total mass loss corresponds to about 85 and 88%).

Table 4
Values, averaged over three tests in a cone calorimeter for two radiation intensities, Q, of the time to ignition, t_i, the rate of heat release, R, the effective heat of combustion, H_c, the total heat evolved, H_e, the total mass loss, M_v, and the and soot mass, M_s (a: average value over the duration of the test, p: peak)

h (kW/m^2)	t_i (s)	R_p (kW/m^2)	R_a (kW/m^2)	$(H_c)_a$ (MJ/kg)	H_e (kJ)	M_v (%)	M_s (kg/kg)($\times 10^4$)
25	4	122	231	14.7	147	80.6	3.6
50	4	36	295	16.6	175	91.5	4.9

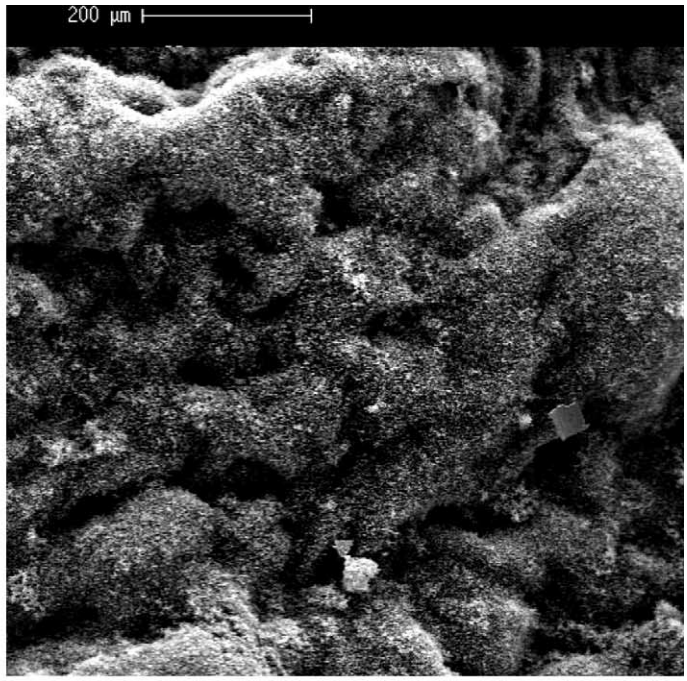

(A)

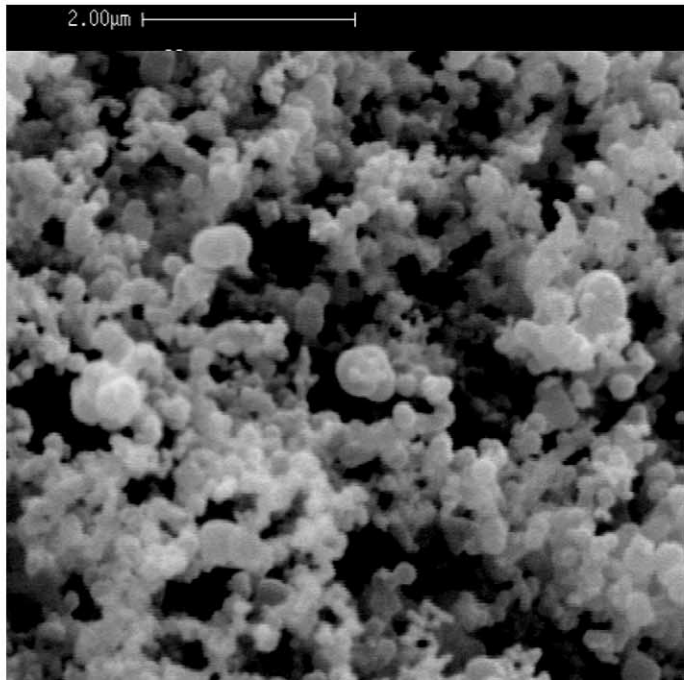

(B)

Fig. 8. (A) SEM micrographs of the surface of the polyurethane foam after exposure to a radiative heat flux of 25 kW/m^2 in a cone calorimeter (100×). (B) SEM micrographs of the surface of the polyurethane foam after exposure to a radiative heat flux of 25 kW/m^2 in a cone calorimeter (125,000×).

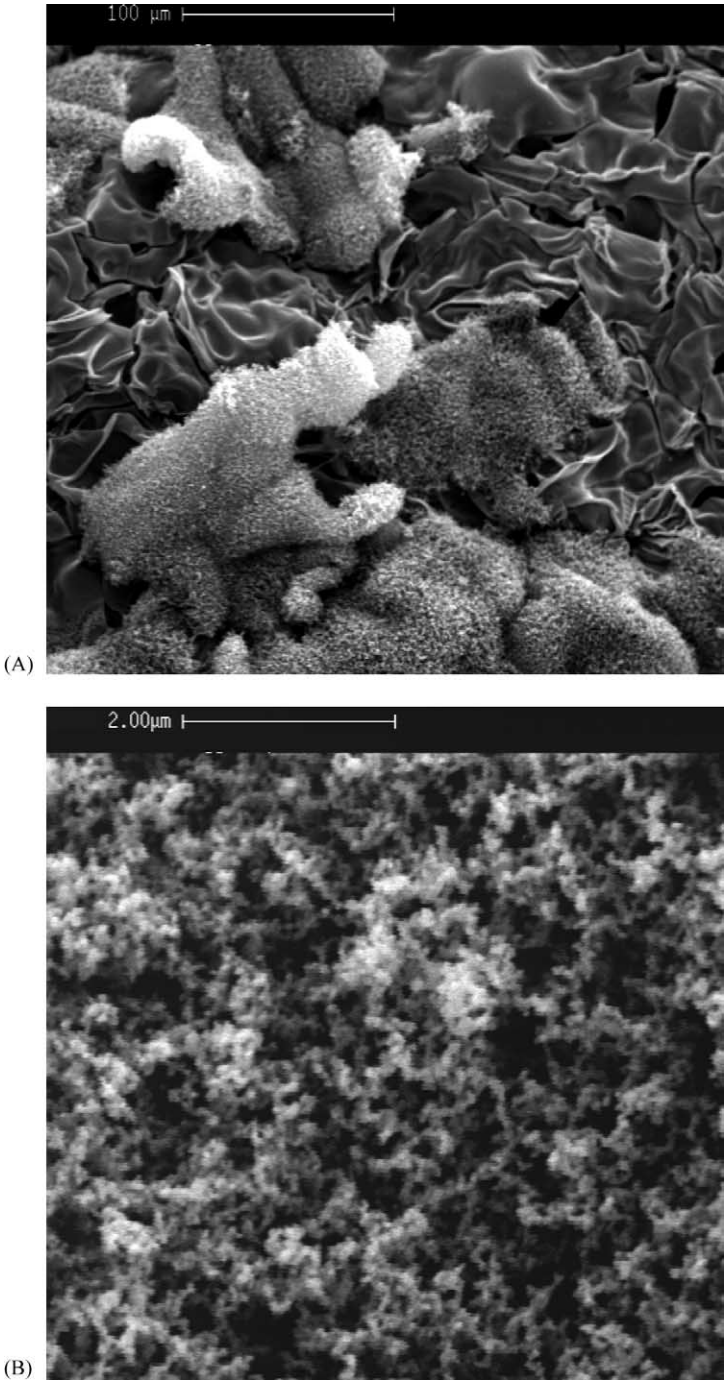

Fig. 9. (A) SEM micrographs of the surface of the polyurethane foam after exposure to a radiative heat flux of 50 kW/m^2 in a cone calorimeter (250×). (B) SEM photograph of the surface of the polyurethane foam after exposure to a radiative heat flux of 50 kW/m^2 in a cone calorimeter (12,500×).

In the former case flame extinction is associated with the termination of the combustion process. However, for the higher external heat flux, once the release of gaseous species lowers to levels unable to sustain a gas-phase flame, a transition occurs to smoldering combustion. The occurrence of this process is also testified by the small, but still significantly different from zero, values of R (about 20 kW/m^2) and carbon monoxide concentration. On the other hand, the scale used in Fig. 7 does not allow the variations in carbon dioxide concentrations to be detected. Smoldering combustion takes place very slowly (up to 500 s, not shown) and gives rise to further solid conversion (about 8%). Consequently, the average value of R is lower for the higher external heat flux. However, in accordance with the higher conversion, the total heat evolved and the effective heat of combustion are higher. Finally, the soot mass detected is also higher.

Combustion at low and high heat fluxes results from the interaction between chemical and physical processes, which should be adequately described by a transport model. The former group comprises both the reactions of the solid phase, discussed here, and the gas-phase combustion of volatile products. The latter corresponds to the transport phenomena of a burning solid and the adjacent gas layer. From the quantitative point of view, the cone calorimeter results can be used for the validation of transport models.

3.3. Morphological changes

It is well known that conduction is a relatively poor mode of heat transfer across insulating materials, such as polyurethane foams. Despite the low temperatures typically established during smolder [8], radiative heat transfer may be controlling. This heat transfer mechanism is often modeled by incorporating an additional terms in the effective thermal conductivity, which is directly proportional to the pore size [20]. Hence, it is important to understand the changes induced by combustion in the morphological structure of the material.

SEM analysis has been applied to specimen obtained for the two radiation intensities considered above, that is, 25 and 50 kW/m^2. For the lower heat flux the charred residue shows a homogeneous structure at the surface (Fig. 8A) consisting of an open network of particles grouped in the form of a chain (Fig. 8B). Particle sizes are generally lower than 100 nm.

The charred residue collected from the 50 kW/m^2 test presents a more compact and fragile structure (Fig. 9A and B). In particular, two different morphological structures can be observed. One part is extremely smooth, without voids or roughness but only slightly corrugated as also shown by very high magnification. The other part presents the same characteristics as those of the low heat flux surface, but particle sizes are even smaller.

From these results, it can be understood that both the conductive and the radiative contribution in the effective thermal conductivity vary with the conversion level of the solid and the severity of the external heating conditions. These features should be adequately taken into account in the formulation of sub-models for the physical properties to be coupled with the conservation equations for process simulation.

4. Conclusions

Thermogravimetric curves of the decomposition of a rigid polyurethane foam in air have been used for the formulation of a reaction mechanism and the estimation of the related kinetic constants, to be used in a transport model. In agreement with previous literature, the process is observed to present three main reaction zones, well described by three first-order reactions with activation energies of 133.6, 81 and 180 kJ/mol.

The thermal response of large samples in a cone calorimeter is significantly affected by the applied radiation intensity both quantitatively (i.e. peak in the rate of heat release, carbon monoxide and carbon dioxide concentration, etc.) and qualitatively. Indeed, for a low heat flux only a relatively short period of flaming combustion is observed, whereas for a high heat flux, the process consists of two stages. The first is again a short-duration flaming combustion, the second very slow smoldering combustion.

The analysis of the SEM micrographs for both low and high radiation intensities indicates that the cellular structure of the foam is completely lost for an open network of lumps consisting of micron-sized particles and/or a smooth slightly corrugated surface. It can be understood that, given the strong reduction in the pore size, the radiative contribution becomes successively less important compared to conduction. These features

should be properly accounted for in the development of a transport model.

Acknowledgements

The research was funded in part by the Italian Space Agency (ASI) under the Contracts I/R/102/00 and I/R/080/01 (Flammability and Smolder of Insulating Materials in Microgravity).

References

[1] J.W. Lyons, The Chemistry and Uses of Fire Retardants, Wiley, New York, 1970.
[2] M.M. Esperanza, A.N. Garcia, R. Font, J.A. Conesa, J. Anal. Appl. Pyrol. 52 (1999) 151.
[3] T.J. Ohlemiller, Prog. Energy Combust. Sci. 11 (1985) 277.
[4] D.A. Schult, B.J. Matkowsky, V.A. Volpert, A.C. Fernandez-Pello, Combust. Flame 101 (1995) 471.
[5] D.P. Stocker, S.L. Olson, D.L. Urban, J.L. Torero, D.C. Walther, A.C. Fernandez-Pello, in: Proceedings of the 26th International Symposium on Combustion, The Combustion Institute, 1996, pp. 1189–1199.
[6] M. Ravey, E.M. Pearce, J. Appl. Polym. Sci. 63 (1997) 47.
[7] T.J. Ohlemiller, J. Bellan, F. Rogers, Combust. Flame 36 (1979) 197.
[8] S.S. Dosanjh, P.J. Pagni, A.C. Fernandez-Pello, Combust. Flame 68 (1987) 131.
[9] D.A. Schult, B.J. Matkowsky, V.A. Volpert, A.C. Fernandez-Pello, Combust. Flame 104 (1996) 1.
[10] R. Bilbao, J.F. Mastral, J. Ceamanos, M.E. Aldea, J. Anal. Appl. Pyrol. 37 (1996) 69.
[11] R. Font, A. Fullana, J.A. Caballero, J. Candela, A. Garcia, J. Anal. Appl. Pyrol. 58–59 (2001) 63.
[12] M. Lanzetta, C. Di Blasi, F. Buonanno, Ind. Eng. Chem. Res. 36 (1997) 542.
[13] C. Di Blasi, C. Branca, Ind. Eng. Chem. Res. 40 (2001) 5547.
[14] C. Di Blasi, C. Branca, G. D'Errico, Thermochim. Acta 364 (2000) 133.
[15] C. Branca, C. Di Blasi, H. Horacek, Ind. Eng. Chem. Res. 41 (2002) 2104.
[16] J. Troitzsch, International Plastics Flammability Handbook, 2nd ed., Hanser, Munich, 1990.
[17] A.W. Benson, C.F. Cullis, Combust. Flame 24 (1975) 217.
[18] G. Varhegyi, M.J. Antal, T. Szekely, P. Szabo, Energy Fuels 3 (1989) 329.
[19] J.A. Conesa, A. Marcilla, J.A. Caballero, R. Font, J. Anal. Appl. Pyrol. 58–59 (2001) 617.
[20] C. Di Blasi, C. Branca, AIChE J. 47 (2001) 2359.